

# Novel Tocopherol Succinate-Polyoxomolybdate Bioconjugate as Potential Anti-Cancer Agent

**Mahnaz Sadat Hosseini**

Student Research Committee, School of Pharmacy and Pharmaceutical Sciences, Isfahan University of Medical Sciences, Isfahan, Iran

**Shaghayegh Haghjooy Javanmard**

Applied Physiology Research Center, Isfahan University of Medical sciences, Isfahan, Iran

**nasim Dana**

Applied Physiology Research Center, Cardiovascular Research Institute, Isfahan University of Medical sciences, Isfahan, Iran

**Laleh Rafiei**

Applied Physiology Research Center, Cardiovascular Research Institute, Isfahan University of Medical sciences, Isfahan, Iran

**Mahboubeh Rostami** (✉ [m.rostami@pharm.mui.ac.ir](mailto:m.rostami@pharm.mui.ac.ir))

Pharmaceutical Sciences Research Center and Department of Medicinal Chemistry, School of Pharmacy and Pharmaceutical Sciences, Isfahan University of Medical Sciences, Isfahan, Iran

<https://orcid.org/0000-0001-9968-821X>

---

## Research Article

**Keywords:** Anderson type Polyoxomolybdate (POMo), Hybrid Organic-Inorganic Bioconjugate, Tocopherol Succinate (TS), Apoptosis, Anti-cancer agent

**Posted Date:** February 11th, 2021

**DOI:** <https://doi.org/10.21203/rs.3.rs-214396/v1>

**License:**  This work is licensed under a Creative Commons Attribution 4.0 International License.

[Read Full License](#)

---

**Version of Record:** A version of this preprint was published at Journal of Inorganic and Organometallic Polymers and Materials on April 24th, 2021. See the published version at <https://doi.org/10.1007/s10904-021-01998-z>.

# Abstract

Up to now, polyoxometalates (POMs) have shown encouraging anti-tumor activities. Unfortunately, the general toxicity with a fateful characteristic has prevented their further clinical application as inorganic drugs. In this study, we synthesized tocopherol succinate-polyoxomolybdate conjugate (T<sub>2</sub>POMo) as a new organic-inorganic hybrid and evaluated its characteristic in-vitro to introduce a safer and more potent POM derivative in the scope of cancer treatment. We synthesized the hybrid via a simple amidation reaction between POMo and tocopherol succinate (TS) using the carbodiimide strategy. The structure was approved by FTIR and HNMR spectroscopy besides the other techniques. The anti-cancer activity was studied on breast cancer cell (MCF-7) and prostate cancer cell (LNCAP) using MTT method and normal cell non-toxicity was checked on Human umbilical vein endothelial cell (HUVEC) using the same protocol, and the flow cytometry technique was used to investigate the apoptosis. The cytotoxicity studies on the breast cancer cell line (MCF-7), prostate cancer cell line (LNCAP) and human umbilical vein endothelial cell (HUVEC) showed that the presence of tocopherol succinate could change and modulate the potency of the final hybrid (IC<sub>50</sub> of 167.3 mg/mL on MCF-7 & 234.1 mg/mL on LNCap respectively). The results showed more cytotoxicity compared to the parent POMo for T<sub>2</sub>POMo conjugation on cancerous cells besides no significant cytotoxicity on normal cells. The flow cytometry results showed that the hybrid conjugation could result in a significant increase in apoptosis (60.88%). So tocopherol succinate bioconjugate of POMo as a novel and potent bioactive POMo could be a promising candidate for further pre-clinical assessments.

## Introduction

Based on the World Health Organization (WHO), cancer is the name of a group of diseases associated with abnormal [cell growth](#) and the potential to attack other parts of the body and one of the leading causes of million deaths worldwide. It was responsible for more than 9 million mortalities in 2018, especially in low to middle-income countries (1).

All of the chemotherapy drugs suffer from some drawbacks, such as high price, numerous side effects, and low bioavailability (2). Thus, it has always been fascinating to find new cytotoxic agents to overcome these limitations by replacing previous drugs in the clinic.

Polyoxometalates (POMs), macroanionic clusters, are chemical structures with early transition metals in which the metal ions in their highest oxidation states are linked together through an oxygen bridge (3). They have been studied in various fields, such as catalysis, material science, pharmaceutical science, medicine, and biosensors because of their unique properties and reactivity (4). During the last decades, POMs have attracted much attention in pharmaceutical research as therapeutic agents like anti-cancers, antibiotics, antivirals, etc. It seems that due to their low price of preparation, simple synthesis, easy modification, and other eminent characteristics, they have a unique chance for being considered as drugs in the future.

Many reports on the anti-cancer activity of POMs and their organic hybrids regardless of the structure, identity, and chemical composition of POMs are available. Even because of their unique potency in this regard, they were introduced as the next generation of metallodrugs by Bijelic et al (5).

Yamase published the first report on the anti-cancer activity of POMs in 1988 around anti-tumor activity (NH<sub>3</sub>Pri)(Mo<sub>7</sub>O<sub>24</sub>) polyoxometalate animal transplantable tumors and human cancer xenograft (6). Still, in the late 20th century, the anti-cancer studies reported by the Sabarinathan team (7) on silicotungstate cluster coordinated organic-inorganic hybrid material [Cu(dmbpy)]<sub>2</sub> [SiW<sub>12</sub>O<sub>40</sub>]·8H<sub>2</sub>O, and Li et al. (8) on Keggin-type rare earth-containing (POMs) specifically in 2019 and 2020 showed the appeal of this research area.

Despite these excellent studies, two significant problems have remained in this regard that impede the clinical application of POMs in cancer therapy; first, compared to other anti-cancer drugs, with an inhibitory concentration (IC<sub>50</sub>) in the nanomolar range, relatively large quantities of POMs are needed to initiate the anti-cancer effect in-vitro and in-vivo. Second, the cytotoxicity in healthy cells and side effects of POMs as a drug should be considered by either increasing the cell-selectivity through targeting strategy, or conjugation to bioactive molecules (3, 9).

Molecular hybridization is expected to open up new interdisciplinary perspectives in medicinal chemistry (10), in most cases, the hybrid compounds benefit from integrating the biological effects of their components. In this regard, combining different pharmacophores, organic or inorganic substructures, is possible with an appropriate rationale to get the desired outcomes.

Hybridization strategy, and specifically the covalent modification, seems to be a valuable strategy to control the inherent cytotoxicity of POMs. This strategy offers additional advantages, including better biological stability and in some cases, better selectivity in POMs (11-13). In this regard, hybridization with some specific bio-molecules, such as peptides, vitamins, proteins, and other bio-ligands have created more research appeal in this kind of cytotoxic agents.

Some of the recent papers on the subject of anti-cancer activity of organic or biological hybrids of POMs are as follows; Boulmier et al in 2017, reported the anti-cancer activity of a series of polyoxometalate-bisphosphonate complexes containing Mo(VI)O<sub>6</sub> octahedra, zoledronate, or an N-alkyl zoledronate analog, in their structures Mn was heterometal. They found promising activities against human non-small cell lung cancer (NCI-H460) cells with IC<sub>50</sub> values for growth inhibition of ~5 μM per bisphosphonate ligand (14).

Hosseini et al. in 2020 reported the cytotoxicity of biotin-conjugated manganese polyoxomolybdate on MCF-7 cell line (IC<sub>50</sub>; 0.082 mM), and HepG2 cell line (IC<sub>50</sub>; 0.091 mM). Meanwhile, they approved the lower cytotoxicity on the HUVEC cell line (15).

Ventura et al. in 2018, reported functionalization of the Anderson-Evans polyoxomolybdate ([MnMo<sub>6</sub>O<sub>24</sub>]<sup>3-</sup>) with a Bombesin antagonist peptide. They studied the anti-cancer activity of this

conjugation against MCF-7, and Hela cell lines, in both cytotoxicity they found IC50 about 75 nM (12).

Vitamin E is well-known as a lipophilic vitamin with anti-oxidant activity, which has also been demonstrated to lower the cancer risk (16). Vitamin E has eight varieties, four tocopherols ( $\alpha$ -,  $\beta$ -,  $\gamma$ - and  $\delta$ -tocopherols) and four tocotrienols ( $\alpha$ -,  $\beta$ -,  $\gamma$ -, and  $\delta$ -tocotrienols), that are particularly promising candidates for the synthesis of anti-cancer hybrid conjugates (17).  $\alpha$ -tocopherol is a significant variant of vitamin E with unique features (18), some of the previous studies revealed that high-dose (100  $\mu$ M)  $\alpha$ -tocopherol, inhibited cell proliferation in ER+ breast cancer, including MCF-7 and T47D cells, in a dose-dependent manner (16, 19).

Among all vitamin E derivatives with unique characteristics, it has been demonstrated that  $\alpha$ -tocopherol succinate (TS) can inhibit the proliferation rate of various cancers in vitro and in vivo (17). Some recent studies have also revealed that  $\alpha$ -TS has anti-cancer activities in various hormone-dependent breast cancers, and even such as MCF-7, MDA-MB-435, 4T1, and MDA-MB-453 cells (16). Furthermore, TS has proven its synergistic effects when it has been used with other therapeutic agents in clinic, in vitro, and in vivo studies (20, 21).

Herein, for the first time following our recent studies and interests, we aimed to evaluate the synergistic effect of  $\alpha$ -TS on the cytotoxicity of an Anderson type polyoxomolybdate (POMo). So, T2POMo conjugation was synthesized using amide covalent bonds, and the cytotoxicity of this novel conjugation was studied on two types of cancerous cell lines besides the normal cells by MTT assay. Furthermore, the apoptosis value was studied quantitatively using Annexin V/propidiumiodide (PI) kit.

## Experimental Section

### - *Materials*

All reagents and solvents were purchased commercially and used without further purification unless specially noted. We used Ultrapure Milli-Q water in all experiments. The 3-(4, 5-dimethylthiazol-2-yl)-2, 5-diphenyltetrazolium bromide (MTT), **tetrabutylammonium bromide (TBAB)**, tris-(hydroxymethyl) aminomethane, N-hydroxysuccinimide (NHS) and 1-Ethyl-3-(3-dimethyl aminopropyl) carbodiimide (EDC) were purchased from Sigma company. Fetal bovine serum (FBS) was purchased from Gibco (Life Technologies AG, Switzerland). Dulbecco's modified Eagle's medium (DMEM) and RPMI- 1640 without folic acid were from Invitrogen Corporation. The breast cancer cell (MCF-7), LNCaP cells (androgen-sensitive human prostate adenocarcinoma cells), and Human umbilical vein endothelial cells (HUVECs) cells were provided from the national cell bank, Pasteur Institute of Iran, and cultured in DMEM (supplemented by 10% FBS). Other remaining chemicals and reagents with required quality were purchased from local vendors.

### - *Synthesis of Compounds*

**Synthesis of POMo**, the synthesis of POMo was achieved in two steps from sodium molybdate and manganese acetate precursors on the basis of our previous study (22).

### **Step 1: Synthesis of [TBA]<sub>4</sub>[ $\alpha$ -Mo<sub>8</sub>O<sub>26</sub>], (POM-1)**

Briefly, a solution of sodium molybdate dihydrate (NaMoO<sub>4</sub>·2H<sub>2</sub>O) (2.50 g, 10.35 mmol) in 6 mL of water was acidified with 6.0 N HCl while stirred vigorously for about 2 mins at an ambient temperature. An aqueous solution of TBAB (1.67 g, 5.20 mmol) was then added to the above solution, white precipitates that were immediately formed were collected and washed respectively with water, ethanol, acetone, and diethyl ether. The product was dissolved in the minimum amount of acetonitrile and stored at -10 °C around 30 h. The bright, colorless, block-shaped crystals were collected and washed with deionized water, ethanol, acetone, and diethyl ether, respectively. The obtained crystals were dried in the vacuum oven overnight, the yield was about 75% based on NaMoO<sub>4</sub> (23).

### **Step 2: Synthesis of ([TBA]<sub>3</sub>[MnMo<sub>6</sub>O<sub>18</sub> ((HOCH<sub>2</sub>)<sub>3</sub>CNH<sub>2</sub>)<sub>2</sub>]); POMo**

A mixture of POM-1, Mn(OAc)<sub>3</sub>·2H<sub>2</sub>O, and (HOCH<sub>2</sub>)<sub>3</sub>CNH<sub>2</sub> (24) (24) was refluxed for 16 h in acetonitrile. The orange solution was cooled to room temperature and filtered to remove impurities, and the orange filtrate was exposed to the diethyl ether for several days (5 days). The POMo was obtained as large orange crystals, were filtered and washed with a small amount of cold acetonitrile and diethyl ether, and then dried in the vacuum (25).

### **Synthesis of Tocopherol succinate POMo conjugate (T<sub>2</sub>POMo)**

$\alpha$ -Tocopheryl succinate (TS) was synthesized based on the procedure reported by Mai et al. (26), by the reaction of  $\alpha$ -Tocopherol and succinic anhydride. TS (0.25 g, 1 mmol), was first activated in the presence of NHS (0.12 g, 1.04 mmol) and EDC (0.19 g, 1.20 mmol) in anhydrous DMF/CH<sub>3</sub>CN, the conjugation between TS and the amine moieties of POMo (0.94 g, 0.5 mmol) was carried out in the presence of catalytic amount of triethylamine for 48 hours in a room temperature. The T<sub>2</sub>POMO bio-conjugation was precipitated by adding diethyl ether, filtered and further purified by acetone and water to remove residual impurities and finally pure product was obtained from acetonitrile (27). The final conjugation was characterized by FTIR, <sup>1</sup>HNMR, and UV-Vis. Spectroscopy, as well as CHNS analysis.

- ***T<sub>2</sub>POMo Stability study***

For this purpose, a solution of T<sub>2</sub>POMo (40  $\mu$ g / mL) was prepared at pH=7.4 in PBS-0.3% DMSO (as close as possible to cell culture media) as reported by Geisberger et al (28). Upon mixing with PBS, the clear solution was retained. The solution was scanned immediately, after 24h, after 48h, and after 72h by UV-Vis spectrophotometer.

#### *- In-vitro Cell Viability Assay*

The cells were cultured in a standard condition of 10% fetal bovine serum (FBS) and 1% penicillin-streptomycin at 37°C in an atmosphere of 5% CO<sub>2</sub>, then were retained in RPMI-1640 (GIBCO) medium for following cytotoxicity evaluation using MTT protocol (29). Typically, stock solutions were prepared in the concentration of 500 mg/mL in phosphate-buffered saline (PBS) (pH 7.4). Cells in a density of 510<sup>3</sup> per well were seeded, then incubated in the same condition as culturing step for 24 h. Different concentrations of POMo, TS, and T<sub>2</sub>POMo (ranging from 50, 100, 200, 300, and 400 µg/mL) were treated regularly on MCF-7, LNCAP, and HUVEC Cells plates. After incubating for 24 h, the medium was removed and 20 µL of MTT solution (5 mg/mL) was added to each well, and incubation was continued for 4h. After that, the medium was replaced with 150 µL DMSO to solubilize the purple formazan precipitates, and the absorbance was read using a microplate reader at 570 nm. The cell viability was calculated using the following equation;

$$\text{Cell Survival \%} = \frac{(A_t - A_b)}{(A_c - A_b)} \times 100$$

in which A<sub>t</sub>, A<sub>b</sub> and A<sub>c</sub> represent mean absorbance of the treatment, blank and negative control, respectively (30). For each treatment, the average of 9 runs was considered, and results were given as Mean ± SD.

#### ***- Hemolysis assay***

The hemocompatibility of POMo, and T<sub>2</sub>POMo were evaluated using a procedure reported by Shi et al (31). Briefly, 1 mL of fresh rat blood was centrifuged at 3000 rpm for about 15 min and precipitated RBCs were isolated and rinsed thoroughly with PBS solution for purification, and stored properly. The hemolysis test solutions of POMo and T<sub>2</sub>POMo, were prepared by adding 40 mL of RBCs to 960 mL of PBS solutions of test groups in different concentrations. The test concentrations were in the range of 50 to 400 mg/mL, the samples were incubated at 37 °C for 6h. After that, the dispersions were centrifuged (3000 rpm, 20 min), and the supernatant was evaluated by UV-visible spectroscopy at 540 nm. The ionized water and PBS were respectively used as positive and negative controls, and the hemolysis ratio was calculated using the following equation:

$$\text{Hemolysis ratio (\%)} = \frac{(A_t - A_n)}{(A_p - A_n)} \times 100$$

In which; A<sub>t</sub>, A<sub>n</sub>, and A<sub>p</sub> refer to absorption of test group, absorption of negative control, and absorption of positive control respectively.

#### ***- Flow cytometry analysis of cell apoptosis***

To approve the apoptosis pathway, the binding proportion of annexin V and propidium iodide uptake was checked using a phosphatidyl serine detection kit (IQ product, Netherlands). In this regard, MCF-7 cells were seeded in a 12-well plate with a density of  $10^4$  cells/well and incubated for 24 h at 37 °C. POMo and T<sub>2</sub>POMo solutions with a concentration of 200 mg/mL were treated on cells and incubation was followed for the next 24 h in the same condition. After that, the cells were washed three times with cold PBS and then harvested using Trypsin. To evaluate the apoptosis ratio, the cells were doubled stained with Annexin-V-FITC and PI respectively according to the manufacturer's proposed procedure and incubated in the dark for 15 min in a room temperature, and analyzed using FACS Calibur flow cytometer. Only single cells were gated for fluorescence analysis (32).

### **- Statistical analysis**

All of the data was analyzed using one-way ANOVA using SPSS software (version of 21) followed by student t-test to evaluate the difference between groups, or by Post Hoc LSD test for more than two groups. The  $p_{\text{value}}$  lower than 0.05 considered as a significant difference between averages.

## **Results And Discussion**

### **- Synthesis of compounds**

[TBA]<sub>4</sub>[α-Mo<sub>8</sub>O<sub>26</sub>] (**POM-1**) was synthesized as the basis for POMo according to the previous reports without any difficulty, after addition of Mn(OAc)<sub>3</sub> and TRIS subunits, [TBA]<sub>3</sub>[MnMo<sub>6</sub>O<sub>18</sub>{(OCH<sub>2</sub>)<sub>3</sub>CNH<sub>2</sub>}<sub>2</sub>] (**POMo**) was isolated as orange crystals in 80% yield from **POM-1** according to the previous reports (25). The reaction of tocopherol succinate with both ends of **POMo** led to the final conjugation **T<sub>2</sub>POMo** as a pale orange powder (figure 1).

Since the synthesis and the characterization of Anderson type polyoxomolybdates (**POM-1 & POMo**) were previously reported, so in this study, the spectral data (1HNMR, FTIR), elemental analysis (CHNS), and XRD pattern were compared with those were reported earlier (25) to ensure about the accurate synthesis of required polyoxometalate subunit. The FTIR, 1HNMR, CHNS data for POM-1 and POMo are as follow, and the XRD pattern for POMo in compared to that report by Marcoux et al. has been provided in figure 2. As it can be seen, the similarity between two patterns of prepared POMo and that retrieved as standard XRD is definite.

[TBA]<sub>4</sub>[α-Mo<sub>8</sub>O<sub>26</sub>] (**POM-1**); FTIR (KBr):  $\nu$  (cm<sup>-1</sup>) 3445 (w, br), 2968(s), 2938 (s), 2875 (s), 1615 (w), 1473 (s), 1371(m), 1339 (w), 1149 (w), 957 (s), 928 (s), 910 (s), 862 (s), 810 (s), 663 (s), 562 (w), 505 (w), 413 (w).

[TBA]<sub>3</sub>[MnMo<sub>6</sub>O<sub>18</sub>(24)2] (**POMo**); FTIR (KBr):  $\nu$  (cm<sup>-1</sup>), 3448 (w, br), 2960 (s), 1479 (s), 1040 (s), 939 (s), 917 (s), 900 (s), 663 (s); 1H-NMR (400 MHz, DMSO-d<sub>6</sub>): 0.94 (t, 36 H), 1.32 (m, 24 H), 1.57 (m, 24 H), 3.12 (m, 24 H), 61.8 (s, 12 H); Elemental analysis: calculated for C<sub>56</sub>H<sub>124</sub>MnMo<sub>6</sub>N<sub>5</sub>O<sub>24</sub>: Elemental Analysis: C

35.73, H6.64, Mn 2.92, Mo 30.59, N 3.72; found experimentally C 35.70 %, H 6.75%, N 3.61, Mn 2.86%, Mo 30.28%; UV-Vis. (CH<sub>3</sub>CN):  $\epsilon_{\text{max}}$ , 220, 254, 356 nm.

The structure of (**T<sub>2</sub>POMo**) were characterized by <sup>1</sup>H-NMR spectroscopy, FTIR spectroscopy, and CHNS elemental analysis as well as UV-vis. spectroscopy, the results are as follow:

### **T<sub>2</sub>POMo bio-conjugate;**

FTIR (KBr):  $\nu$  (cm<sup>-1</sup>) 3489 (w, br), some medium weight bands below 3000 cm<sup>-1</sup>, 1741.8 (m, ester C=O of TS), 1688.7 (m, newly formed amide C=O), 1479 (m), 1041 (s), 939 (s), 917 (s), 662 (s).

<sup>1</sup>H-NMR (400 MHz, DMSO-*d*<sub>6</sub>): 0.96 (t, 36 H, POMo), 1.32 (m, 24 H, POMo), 1.56 (m, 8 H, TS), 1.69 (m, 4H, TS), 1.72 (m, 24 H, POMo), 3.16 (m, 24 H, POMo), 3.34-342 (m, 6 H, TS), 4.15 (s, 2H, TS), 4.30 (s, 2H, TS), 6.38 (m, 4H, TS), 9.38 (bs, 2H, newly formed amide NH), 61.60 (s, 12 H, POMo);

Elemental analysis:

calculated for C<sub>122</sub>H<sub>230</sub>MnMo<sub>6</sub>N<sub>5</sub>O<sub>32</sub>: C, 50.36 %; H, 7.97 %; N, 2.41 %; Mn, 1.89 %; Mo, 19.79 %

found experimental C, 50.10 %; H, 8.05 %; N, 2.49 %, Mn, 1.81 %; Mo, 19.65 %.

UV-Vis. (CH<sub>3</sub>CN): 207, 224, 256, 293, 388 nm.

Based on the available reports, six edge-sharing MoO<sub>6</sub> octahedral are arranged around a core of the MnO<sub>6</sub> unit, making the Anderson structure. The TRIS are bound to the Mn(III) ion in the core via its alkoxy groups, so two amine groups of TRIS are oriented to outside of POM and are available for further modification The organic groups cover both sides of the planar hexagon through the chemical bonding to the amine groups of TRIS (25).

As can be seen in Figure 1, we used both amine groups of POMo for the functionalization with TS. The amidation reaction between the carboxylic acid of TS with POMOs was carried out through the carbodiimide strategy using EDC/NHS (33). Purification through precipitation afforded the final product with a relatively high yield. The chemical structure of the T<sub>2</sub>POMo conjugation was confirmed by elemental analysis, FT-IR spectroscopy, and <sup>1</sup>H NMR spectroscopy. With an in-depth look at FTIR spectrum (figure 3) of final conjugation compared to the POMo, we find some changes after the conjugation, for example, N-H stretching frequency has increased to some extent from 3448 cm<sup>-1</sup> to 3489 cm<sup>-1</sup>, the carbonyl group stretching frequency moves from 1719 cm<sup>-1</sup> in TS to 1688 cm<sup>-1</sup> in T2POMo due to the conjugation, we also see the primarily ester band of TS in the related place around 1741 cm<sup>-1</sup>. Finally, some spectral details related to TS have been appeared in corresponding area in final conjugation spectra. Furthermore, we can see the characteristic bands of Anderson-type POMo in proper regions around 939.2, 917.7, and 662.8 cm<sup>-1</sup> respectively after conjugation with TS. These IR proofs undoubtedly supported the correct amide formation between TS and POMo.

The data of  $^1\text{H}$ NMR of T2POMo is the best complementary one, the all fundamental signals of TBA and TRIS in the POMo scaffold are relocated intact in T<sub>2</sub>POMo. As shown by Marcoux et al. (25), because of strong electron-withdrawing identity of POM, its methylene protons (belong to TRIS) are appeared around 60-62 ppm in  $^1\text{H}$ NMR spectra with the right signal ratio to other related peaks. Along characteristic signals of TS and POMo, the signal of NH amide was correctly appeared around 8.6 ppm with the exact signal ratio to the POMo CH<sub>2</sub> moieties around 61 ppm (as shown in figure 4). Based on these spectral proofs, the conjugation of two molecules of TS to POMo scaffold was approved initially. The best complementary evidence was obtained from elemental analysis, according to these results and comparing with theoretical values, the chemical structure and formula were approved finally (25). Furthermore, UV-vis. spectroscopy (figure 5), showed the characteristic bands for both of TS and POMo accordingly, it seems that upon the conjugation, the shape and details of the spectrum have changed completely in comparison to its sub-groups (TS & POMo). The general shape of the bio-conjugate (T2POMo) spectrum confirms the combination of the two components as well. There are some small changes in maximum absorption wave length of components which are in line with those reported by others for hybrid organic-inorganic conjugations (34).

- ***Stability of T<sub>2</sub>POMo conjugate***

Before *in vitro* cytotoxicity evaluation, the stability of the T2POMo conjugation should be checked in the same condition as MTT assay protocol. In this regard, the stability of T2POMo conjugation was analyzed using the UV-Vis. spectrum of the dissolved sample after specified times (instantly, 24h, 48h, and 72h after) (35, 36).

The UV/vis spectrum of T2POMo in PBS (Figure 6) clearly indicates its stability around neutral pH conditions through monitoring of the characteristic of POM absorption bands, i.e.

The characteristic of T2POMo absorption bands did not undergo significant changes at any wavelength over a period of 3 days. These results agree well with the previously observed stability which was reported by Geisberger et al (28).

### ***In vitro* Cytotoxicit Assessments (MTT assay)**

To study the effect of TS conjugation on the cytotoxicity profile of POMo in final product, two cancer cell lines comprising MCF-7 and LNCAP were selected due to their relatively high level of tocopherol receptor on them based on previous reports (37, 38). The cells were treated with different concentrations ranging from 50 – 400 mg/mL of TS, POMo and T2POMo. Furthermore, the normal cell cytotoxicity was evaluated on human umbilical vein endothelial cells (HUVEC) in the same way using a concentration of 400 mg/mL.

The results of *in vitro* cytotoxicity for the final conjugation (T2POMo) in comparison to the POMo and TS, on the MCF-7, LNCAP, and HUVEC cells are presented in figures (7, 8 and 9). Figure 7 represents the cytotoxicity profile of T<sub>2</sub>POMo in two different incubation times and different concentrations on MCF-7

cell line. As it can be seen, the cytotoxicity profile is fully time and dose responsive ( $p < 0.05$  for each comparing). Based on these initial results, we selected the 24h for incubation time and the comparative cytotoxicity of POMo and T2POMo have been evaluated on both of MCF-7 and LNCaP cell lines (figure 8). Eventually, Figure 9 represents the comparative cytotoxicity of POMo and T<sub>2</sub>POMo on the HUVEC normal cells.

Previous reports have been repeatedly referred to the anti-cancer properties of TS, and the synergistic effects of TS on the cytotoxic properties of some anti-cancer drugs and agents (17). So it seems that TS is a good candidate for enhancing the anti-cancer properties and based on these studies, TS was selected to bind to polyoxomolybdate.

As can be deduced from figure 8 (up), T2POMo exhibited considerably a better growth inhibition effect on MCF-7 cells compared to POMo and TS. The IC<sub>50</sub> of the T2POMo and POMo on MCF-7 were 167.3 mg/mL and 321.7 mg/mL respectively. On the other hand, both of POMo and T2POMo showed somewhat less cytotoxic effects on LNCAP (figure 8 down), the IC<sub>50</sub> of T2POMo and POM on the LNCAP were respectively 234.1 mg/mL and 382.2 mg/mL estimated. The better detected activity on MCF-7 could be attributed to the higher value of tocopherol responsivity in this type of cells as human protein atlas implied (39).

However, the complementary and adjuvant effects of TS on the cytotoxicity effects in both cell lines are well evident and the main hypothesis of this study seems to be confirmed.

The second hypothesis of this study was to reduce the cytotoxicity effects on HUVEC normal cells, which is confirmed by the results of normal cell line (figure 7).

The protective effects of tocopherol, mentioned earlier (40), appear to help reduce toxicity on the normal cell line. The cytotoxicity of T2POMo and POMo were evaluated on the HUVEC cells at the concentration of 400 mg/mL, which was high enough to see the cytotoxic effects. Interestingly, we did not get any considerable cytotoxicity on HUVEC in comparison to the positive control (cis-platin) at the same concentration for T2POMo. As seen in **Figure 8**, both POMo and T2POMo have higher cell viability compared to the cis-platin at the same concentration (\* and \$ mean significant difference between each groups and positive control), and this effect is recognized much profoundly in the case of T2POMo comparing Cis-Platin ( $p_{\text{value}} < 0.05$ ). Furthermore, there are significant difference between all treating groups and control group with 100% of viability (@ means significant difference with control).

The more cytotoxicity of T2POMo compared to the POMo, can be a result of the inherent toxicity of the POMo, besides its facilitated cell entry through tocopherol receptors. In other words, the cytotoxicity of the T2POMo was improved by higher cell endocytosis of the conjugation through the tocopherol receptors. Although the cellular behavior of T2POMo is not precisely apparent, we find the better activity of the conjugation against the MCF-7 cancerous cells than the LNCAP ones. This lower effect on LNCAP cell lines can be explained by the lower expression level of tocopherol-binding proteins on LNCAP cells, or probably, the lower sensitivity of the LNCAP cells compared to the MCF-7 cells in the culturing process or

other intracellular mechanisms that are predominant in MCF-7 cells relative to the LNCAP ones. Based on the evidence obtained from the Human Protein Atlas database, the MCF-7 tumor cells have more expression of the tocopherol-binding protein (HLCS gene) than the prostate tumor cells; then, we can attribute the observed results to this fact (41).

### ***-Hemolysis assay***

The evaluation of possible toxicity in red blood cells (RBC), with measuring the rate of hemolysis, is the best initial biological assay among the different cytotoxicity assays. This assay is based on red cell membrane rupturing in the presence of any xenobiotic. RBC are the main cells in blood circulation which xenobiotics encounter initially following intravenous injection. Thus, any interruption in the membrane of RBC would certainly disrupt their vital function, and could be lethal (42). The haemolytic activity of the POMo and its bioconjugation T<sub>2</sub>POMo (figure 9) was evaluated in erythrocytes from rat employing standard methodology. The subsequent release of haemoglobin was used to assess haemolytic activity as the function of concentration, with concentrations ranging from 50 to 400 µg/mL. Based on obtained results, in all concentrations, the T<sub>2</sub>POMo conjugation is significantly safer (Pvalue <0.05) than the POMo even at 400 mg/mL. This safety is profoundly apparent in higher concentrations, and as it can be seen even at a concentration of 400 mg/mL the total percent of hemolysis is still below 5 percent in the case of T<sub>2</sub>POMo which is the promising outcome (31). It seems that for both POMo and T<sub>2</sub>POMo the best concentration for being safe to RBC is 200 mg/mL.

### **-Apoptosis quantification using flowcytometry protocol**

To quantify the cell apoptosis, MCF-7 cells (the better cytotoxic effects were obtained on it) were treated with the same concentration of both POMo and T<sub>2</sub>POMo (200 mg/mL), incubated for 24h, and finally were stained by Annexin V/propidiumiodide (PI). The Annexin V binds to cells in early apoptosis stage, which can be used as a very specific apoptotic marker and PI stains cells in late apoptosis and dead cells (43). The results have been shown in figure 10, the upper left quadrant shows the percent of necrosis in cell death, the upper right shows late apoptotic cells, the lower left shows normal alive cells and the lower right quadrant shows the cells in early apoptosis stage. The results showed that the proportion of apoptotic cells (in early and late phase) increased by the addition of POMo and T<sub>2</sub>POMo to 36.56%, and 60.88 % respectively. The proportion of late apoptotic cells induced by the T<sub>2</sub>POMo is significantly higher than the POMo (18.36 % vs. 5%), and more profoundly increased regarding the control group (2.88%).

So, it can be concluded that the conjugation of TS to the POMo improved the cytotoxicity of POMo through the valuable mechanism of programmed cell death. The same results have been reported by peers in this area (32).

Finally, as Zamolo *et al.* have stated, this approach provides an efficient cytotoxic bioactive inorganic agent and paves the way to bio-functionalization of the POMs for bio-recognition, cell internalization and biomimetic catalysis (44).

This result always is promising for a new cytotoxic compound, reducing the side effects or improving the biocompatibility accompanying by the better cytotoxicity profile.

## Conclusion

Achieving new cytotoxic agents with improved effects compared to previous generations has always been the focus of chemists in the field of medicine. Polyoxometalates are considered as the next generation of inorganic anti-cancer compounds, so designing and the synthesis of hybrid conjugations of these compounds using bioactive molecules can be a promising path for further development. In this study, a new generation of polyoxomolybdate hybrid conjugation was evaluated. Preliminary in vitro cytotoxicity results showed that polyoxomolybdate conjugation with tocopherol succinate could increase cytotoxicity on cancer cells and reduce cell toxicity on normal healthy cells. Also, it seems that tocopherol can facilitate the entry of polyoxomolybdate into the cell and besides create synergistic anti-cancer effects.

This synergistic effect can be related to the targeting ability of the tocopherol and the intrinsic cytotoxicity of the POMo. As a complementary fact, the designed hybrid conjugation of polyoxomolybdate and tocopherol succinate showed a significantly improved apoptosis compared to peer polyoxomolybdate which is the valuable outcome of this study.

Our preliminary findings in this study convinced to continue to synthesis bioactive POMs with enhanced anti-tumor properties.

## Declarations

### ACKNOWLEDGEMENTS

We acknowledge the financial support of Pharmaceutical Sciences Research Center, School of Pharmacy and Pharmaceutical Sciences, Isfahan University of Medical Sciences, grant number; 297079.

### CONFLICTS OF INTEREST

The authors declare that they have no conflicts of interest.

## References

1. WHO. <https://www.who.int/news-room/fact-sheets/detail/cancer> 2018
2. Dickens E, Ahmed S. Principles of cancer treatment by chemotherapy. Surgery (Oxford). 2018;36(3):134-8.
3. Yang H-K, Cheng Y-X, Su M-M, Xiao Y, Hu M-B, Wang W, et al. Polyoxometalate–biomolecule conjugates: A new approach to create hybrid drugs for cancer therapeutics. Bioorg. Med. Chem. Let. 2013;23(5):1462-6.

4. Karimian D, Yadollahi B, Mirkhani V. Dual functional hybrid-polyoxometalate as a new approach for multidrug delivery. *Micropor. Mesopor. Mat.* 2017;247:23-30.
5. Bijelic A, Aureliano M, Rompel A. Polyoxometalates as potential next-generation metallodrugs in the combat against cancer. *Ang. Chem. Int. Ed.* 2019;58(10):2980-99.
6. Yamase T, Fujita H, Fukushima K. Medical chemistry of polyoxometalates. Part 1. Potent antitumor activity of polyoxomolybdates on animal transplantable tumors and human cancer xenograft. *Inorg. Chim. Acta.* 1988;151(1):15-8.
7. Sabarinathan C, Karthikeyan M, Harisma BR, Murugappan RM, Arumuganathan T. One Pot Synthesis of Luminescent Polyoxometalate Supported Transition Metal Complex and biological evaluation as a potential larvicidal and anti-cancer agent. *J. Mol. Struc.* 2020;1206:127486.
8. Li X-H, Chen W-L, Li Y-G, He P, Di Y, Wei M, et al. Multi-functional rare earth-containing polyoxometalates achieving high-efficiency tumor therapy and visual fluorescence monitoring. *Inorg. Chem. Commun.* 2019;104:40-7.
9. Song Y-F, McMillan N, Long D-L, Kane S, Malm J, Riehle MO, et al. Micropatterned surfaces with covalently grafted unsymmetrical polyoxometalate-hybrid clusters lead to selective cell adhesion. *J. Am. Chem. Soc.* 2009;131(4):1340-1.
10. Geisberger G, Paulus S, Gyenge EB, Maake C, Patzke GR. Targeted delivery of polyoxometalate nanocomposites. *Small.* 2011;7(19):2808-14.
11. Zhao H, Tao L, Zhang F, Zhang Y, Liu Y, Xu H, et al. Transition metal substituted sandwich-type polyoxometalates with a strong metal–C (imidazole) bond as anticancer agents. *Chem. Commun.* 2019;55(8):1096-9.
12. Ventura D, Calderan A, Honisch C, Krol S, Serrati S, Bonchio M, et al. Synthesis and biological activity of an Anderson polyoxometalate bis-functionalized with a B ombesin-analog peptide. *Pept. Sci.* 2018;110(5):e24047.
13. Li M, Xu C, Wu L, Ren J, Wang E, Qu X. Self-Assembled Peptide–Polyoxometalate Hybrid Nanospheres: Two in One Enhances Targeted Inhibition of Amyloid  $\beta$ -Peptide Aggregation Associated with Alzheimer's Disease. *Small.* 2013;9(20):3455-61.
14. Boulmier A, Feng X, Oms O, Mialane P, Rivière E, Shin CJ, et al. Anticancer activity of polyoxometalate-bisphosphonate complexes: Synthesis, characterization, in vitro and in vivo results. *Inorg. Chem.* 2017;56(13):7558-65.
15. Hosseini MS, Javanmard SH, Rafiei L, Hariri AA, Dana N, Rostami M. Anti-Cancer Activity of Biotin-Polyoxomolybdate Bioconjugate. *Eur. J. Med. Oncol.* 2020;4(1):42.
16. Wei CW, Yu YL, Chen YH, Hung YT, Yiang GT. Anticancer effects of methotrexate in combination with  $\alpha$ -tocopherol and  $\alpha$ -tocopherol succinate on triple-negative breast cancer. *Oncol. Rep.* 2019;41(3):2060-6.
17. Duhem N, Danhier F, Pourcelle V, Schumers J-M, Bertrand O, LeDuff CcS, et al. Self-assembling doxorubicin–tocopherol succinate prodrug as a new drug delivery system: synthesis, characterization, and in vitro and in vivo anticancer activity. *Bioconjug. Chem.* 2014;25(1):72-81.

18. Orabi SA, Abdelhamid MT. Protective role of  $\alpha$ -tocopherol on two *Vicia faba* cultivars against seawater-induced lipid peroxidation by enhancing capacity of anti-oxidative system. *J. Saudi Soc. Agricul. Sci.* 2016;15(2):145-54.
19. Mamede AC, Tavares SD, Abrantes AM, Trindade J, Maia JM, Botelho MF. The role of vitamins in cancer: a review. *Nutr. Cancer.* 2011;63(4):479-94.
20. Liu B, Han L, Liu J, Han S, Chen Z, Jiang L. Co-delivery of paclitaxel and TOS-cisplatin via TAT-targeted solid lipid nanoparticles with synergistic antitumor activity against cervical cancer. *Int. J. Nanomed.* 2017;12:955.
21. Mehata AK, Bharti S, Singh P, Viswanadh MK, Kumari L, Agrawal P, et al. Trastuzumab decorated TPGS-g-chitosan nanoparticles for targeted breast cancer therapy. *Colloid. Surf. B: Biointerfaces.* 2019;173:366-77.
22. Hosseini MS, Javanmard SH, Rafiei L, Hariri AA, Dana N, Rostami M. Anti-Cancer Activity of Biotin-Polyoxomolybdate Bioconjugate. *EJMO.*2020.
23. Ginsberg AP. *Inorg. Syn.* John Wiley & Sons; 1990.
24. Calabrese G, Nesnas JJ, Barbu E, Fatouros D, Tsibouklis J. The formulation of polyhedral boranes for the boron neutron capture therapy of cancer. *Drug Discov. Today.* 2012;17(3):153-9.
25. Marcoux PR, Hasenknopf B, Vaissermann J, Gouzerh P. Developing remote metal binding sites in heteropolymolybdates. *Eur. J. Inorg. Chem.* 2003;2003(13):2406-12.
26. Ni J, Mai T, Pang S-T, Haque I, Huang K, DiMaggio MA, et al. In vitro and in vivo anticancer effects of the novel vitamin E ether analogue RRR- $\alpha$ -tocopheryloxybutyl sulfonic acid in prostate cancer. *Clin. Cancer Res.* 2009;15(3):898-906.
27. Vashist SK. Comparison of 1-ethyl-3-(3-dimethylaminopropyl) carbodiimide based strategies to crosslink antibodies on amine-functionalized platforms for immunodiagnostic applications. *Diagnostics.* 2012;2(3):23-33.
28. Geisberger G, Gyenge EB, Hinger D, Bösiger P, Maake C, Patzke GR. Synthesis, characterization and bioimaging of fluorescent labeled polyoxometalates. *Dalton Trans.* 2013;42(27):9914-20.
29. Morgan DM. Tetrazolium (MTT) assay for cellular viability and activity. *Polyamine protocols:* Springer; 1998. p. 179-84.
30. Freshney RI. Culture of specific cell types. *Culture of animal cells: a manual of basic technique.* 2005.
31. Shi Y, Yin J, Peng Q, Lv X, Li Q, Yang D, et al. An acidity-responsive polyoxometalate with inflammatory retention for NIR-II photothermal-enhanced chemodynamic antibacterial therapy. *Biomater. Sci.* 2020;8(21):6093-9.
32. Fu L, Gao H, Yan M, Li S, Li X, Dai Z, et al. Polyoxometalate-Based Organic–Inorganic Hybrids as Antitumor Drugs. *Small.* 2015;11(24):2938-45.
33. Liang N, Sun S, Li X, Piao H, Piao H, Cui F, et al.  $\alpha$ -Tocopherol succinate-modified chitosan as a micellar delivery system for paclitaxel: Preparation, characterization and in vitro/in vivo evaluations. *Int. J. Pharm.* 2012;423(2):480-8.

34. Xu B, Wei Y, Barnes CL, Peng Z. Hybrid molecular materials based on covalently linked inorganic polyoxometalates and organic conjugated systems. *Ang. Chem. Int. Ed.* 2001;40(12):2290-2.
35. Gumerova NI, Rompel A. Polyoxometalates in solution: Speciation under spotlight. *Chem. Soc. Rev.* 2020, 49, 7568-7601.
36. Blazevic A, Al-Sayed E, Roller A, Giester G, Rompel A. Tris-Functionalized Hybrid Anderson Polyoxometalates: Synthesis, Characterization, Hydrolytic Stability and Inversion of Protein Surface Charge. *Chem. A Eur. J.* 2015;21(12):4762-71.
37. Sylvester PW, Shah SJ. Mechanisms mediating the antiproliferative and apoptotic effects of vitamin E in mammary cancer cells. *Front .Biosci.* 2005;10(1-3):699.
38. Pierpaoli E, Viola V, Pilolli F, Piroddi M, Galli F, Provinciali M.  $\gamma$ - and  $\delta$ -tocotrienols exert a more potent anticancer effect than  $\alpha$ -tocopheryl succinate on breast cancer cell lines irrespective of HER-2/neu expression. *Life Sci.* 2010;86(17-18):668-75.
39. atlas thp. RNA cell line categoryi : Cell line enhanced (GAMG, SK-BR-3, T-47d, U-2 OS, U-2197 [Available from: <https://www.proteinatlas.org/ENSG00000137561-TTPA/cell#rna>.
40. Zhu Q-X, Shen T, Ding R, Liang Z-Z, Zhang X-J. Cytotoxicity of trichloroethylene and perchloroethylene on normal human epidermal keratinocytes and protective role of vitamin E. *Toxicology.* 2005;209(1):55-67.
41. <https://www.proteinatlas.org/ENSG00000159267-HLCS>.
42. Pagano M, Faggio C. The use of erythrocyte fragility to assess xenobiotic cytotoxicity. *Cell Biochem. Funct.* 2015;33(6):351-5.
43. Riccardi C, Nicoletti I. Analysis of apoptosis by propidium iodide staining and flow cytometry. *Nat. Protoc.* 2006;1(3):1458-61.
44. Zamolo VA, Modugno G, Lubian E, Cazzolaro A, Mancin F, Giotta L, et al. Selective Targeting of Proteins by Hybrid Polyoxometalates: Interaction Between a Bis-Biotinylated Hybrid Conjugate and Avidin. *Front. Chem.* 2018;6:278-88.

## Figures

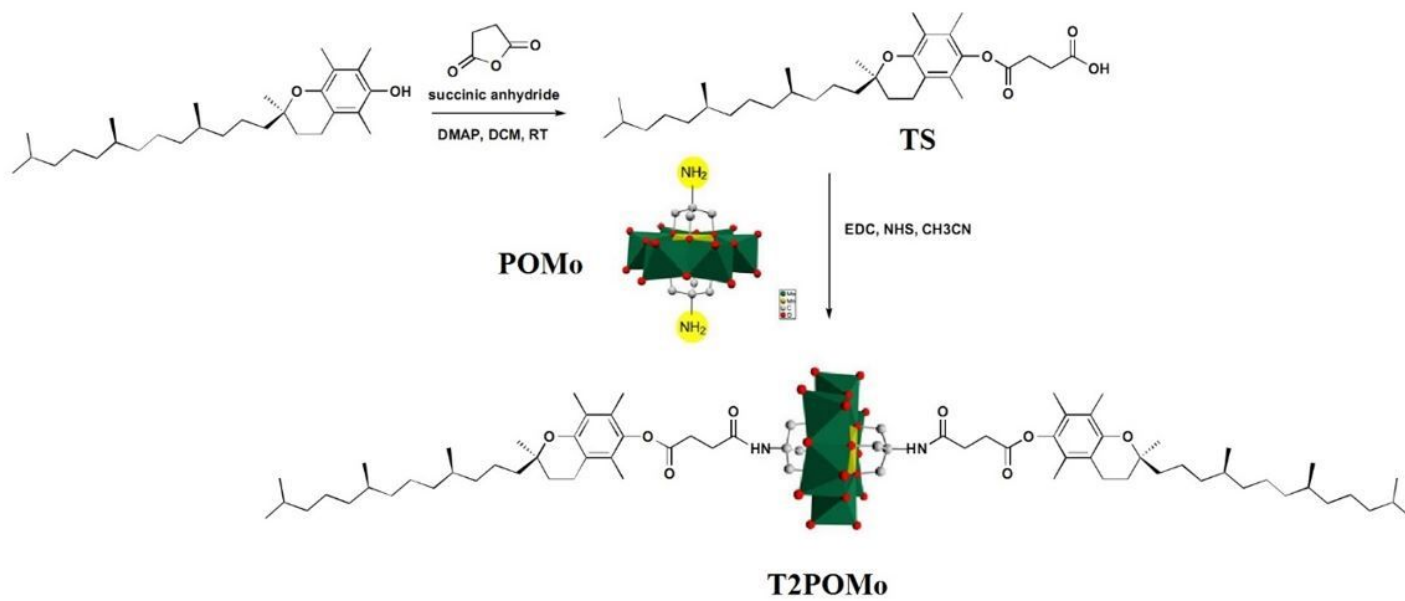


**Figure 1**

the schematic view of Tocopherol-POM conjugate (T2POMo) synthesis

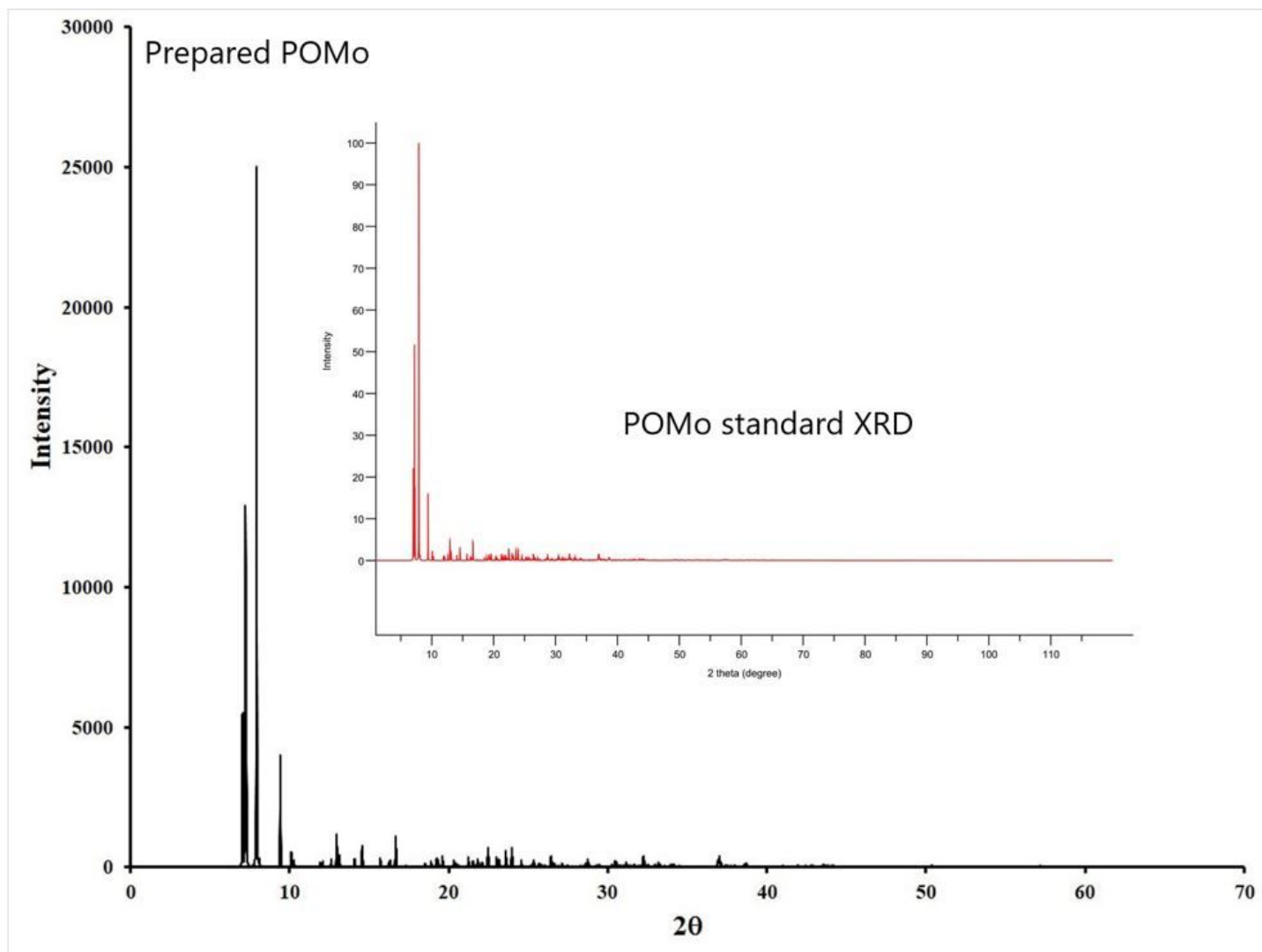


**Figure 2**

XRD pattern for prepared POMo in compare to standard pattern The standard pattern was retrieved from CIF file that received from Cambridge Crystallographic Data Centre for Pierre R. Marcoux et al. reference paper(25).

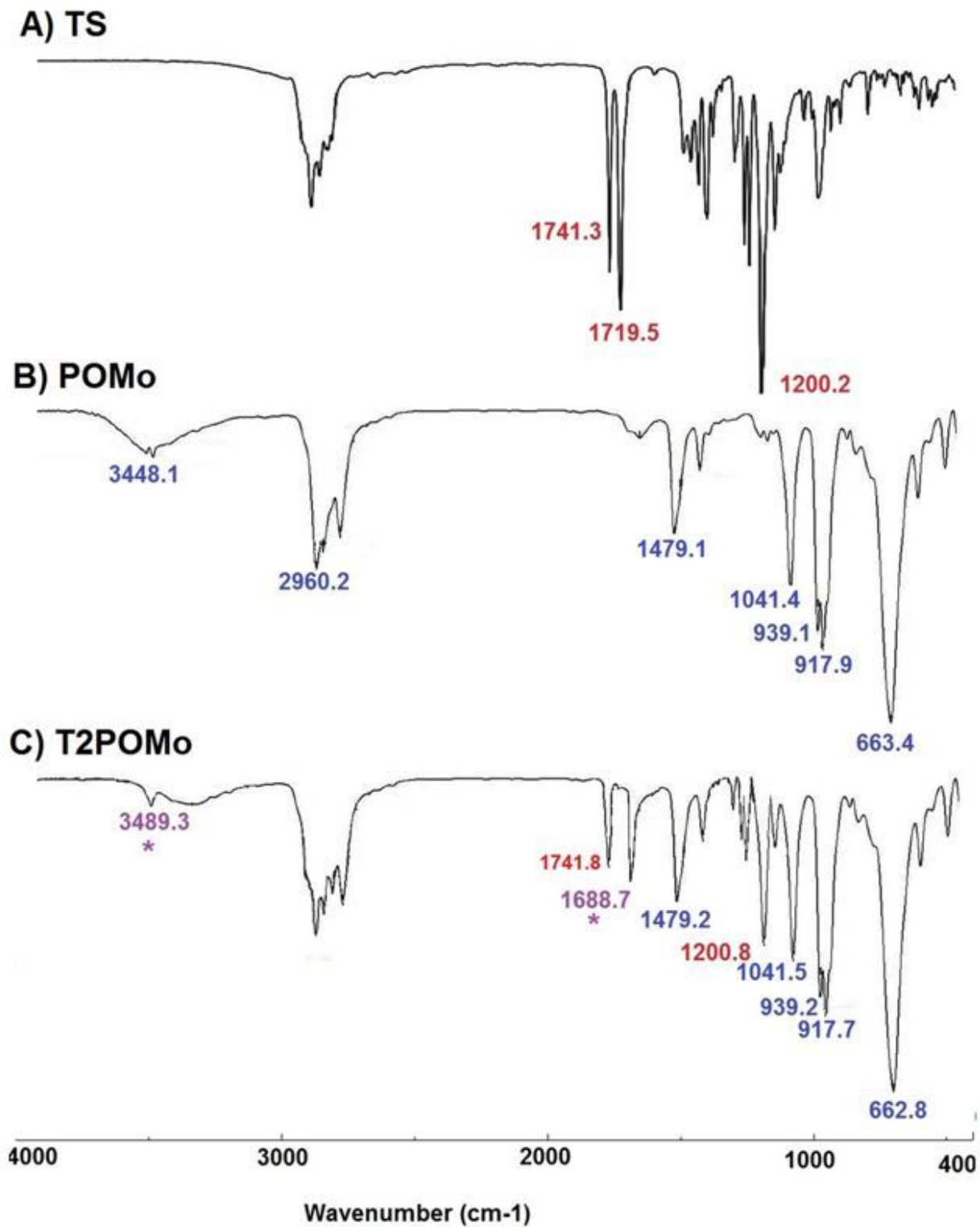


Figure 3

FTIR Spectrum of final T2POMo conjugate

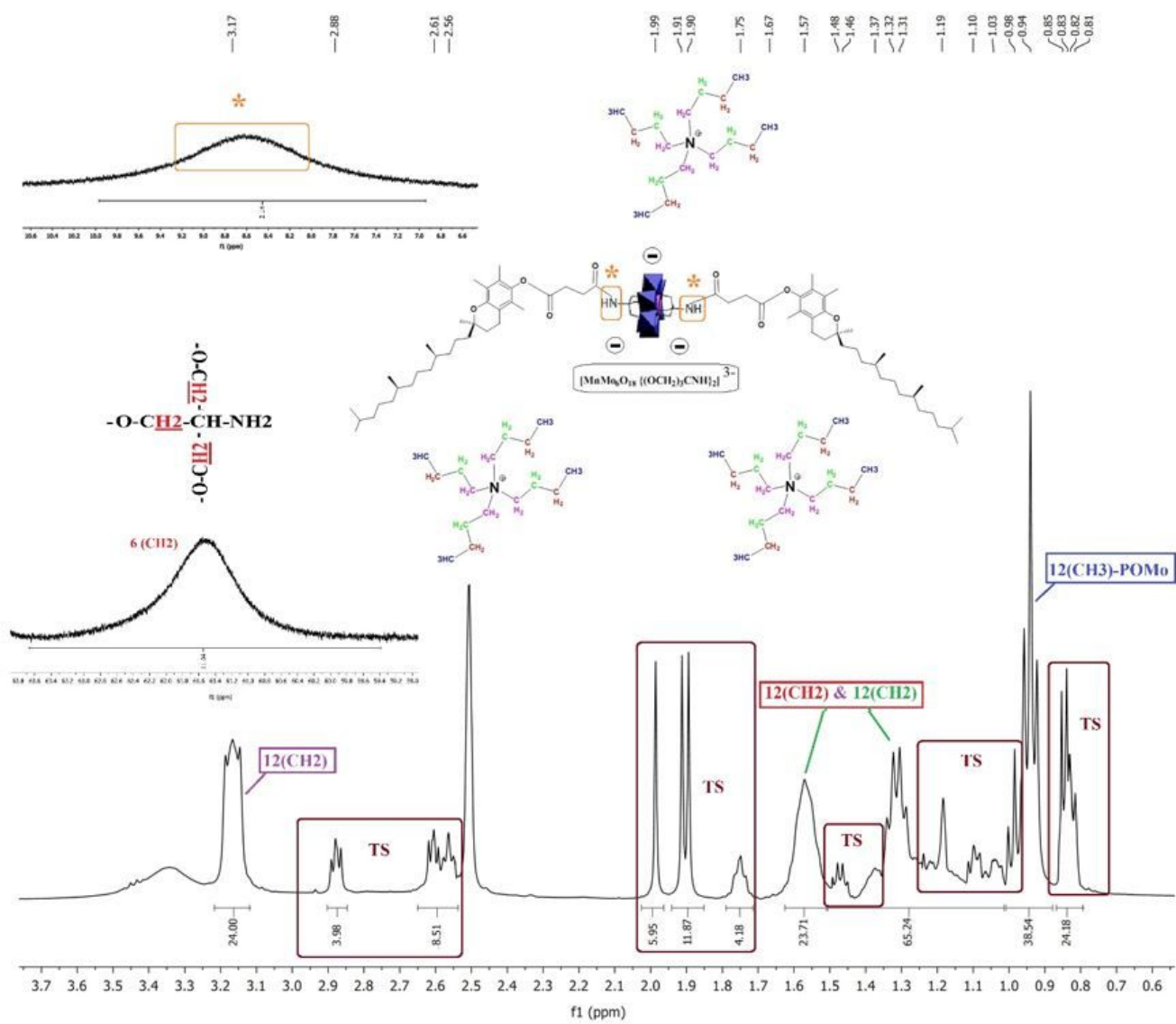


Figure 4

<sup>1</sup>H NMR spectra for T2POMo conjugate

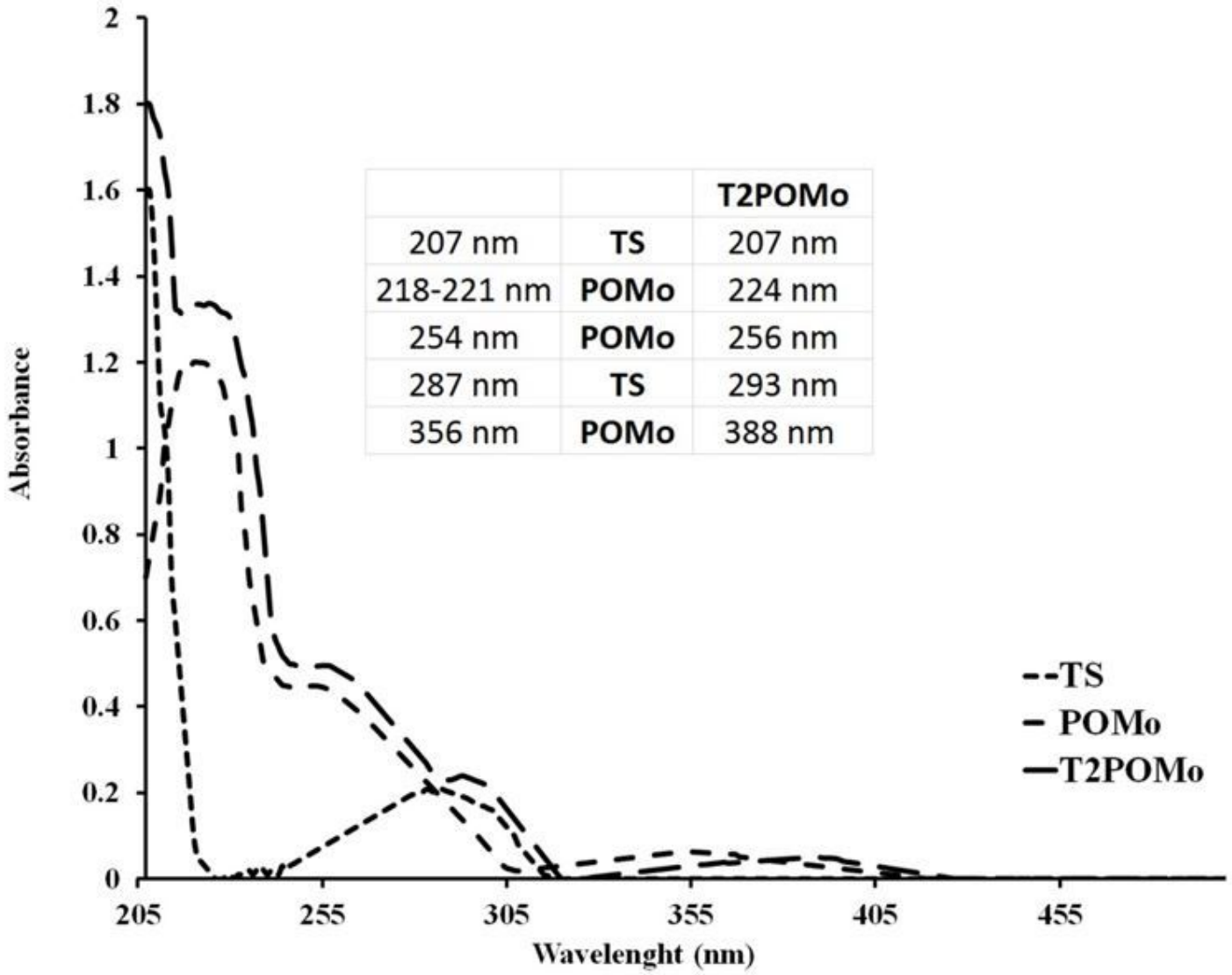


Figure 5

UV-Vis. Spectra for T2POMo and its related sub-units (TS & POMo)

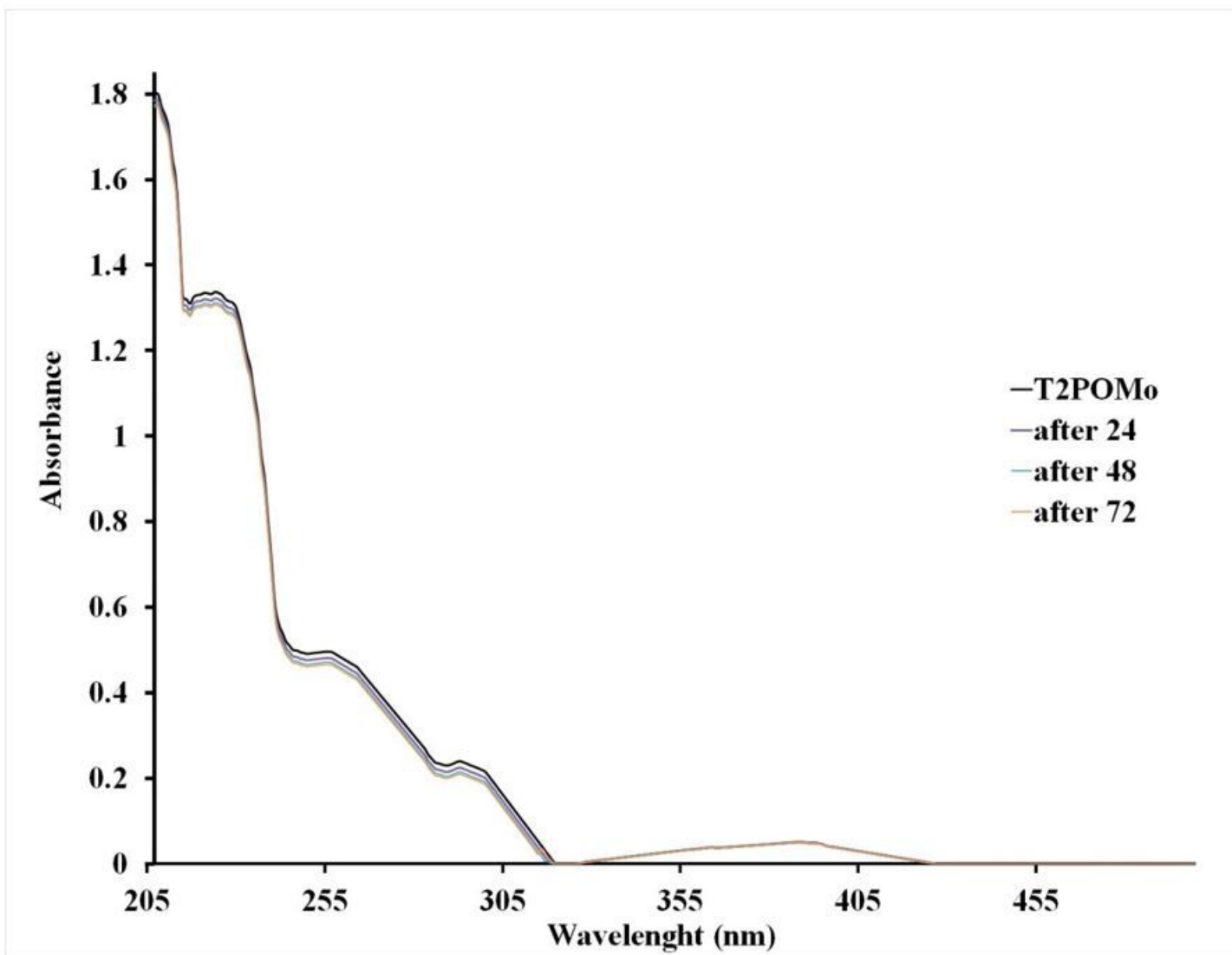
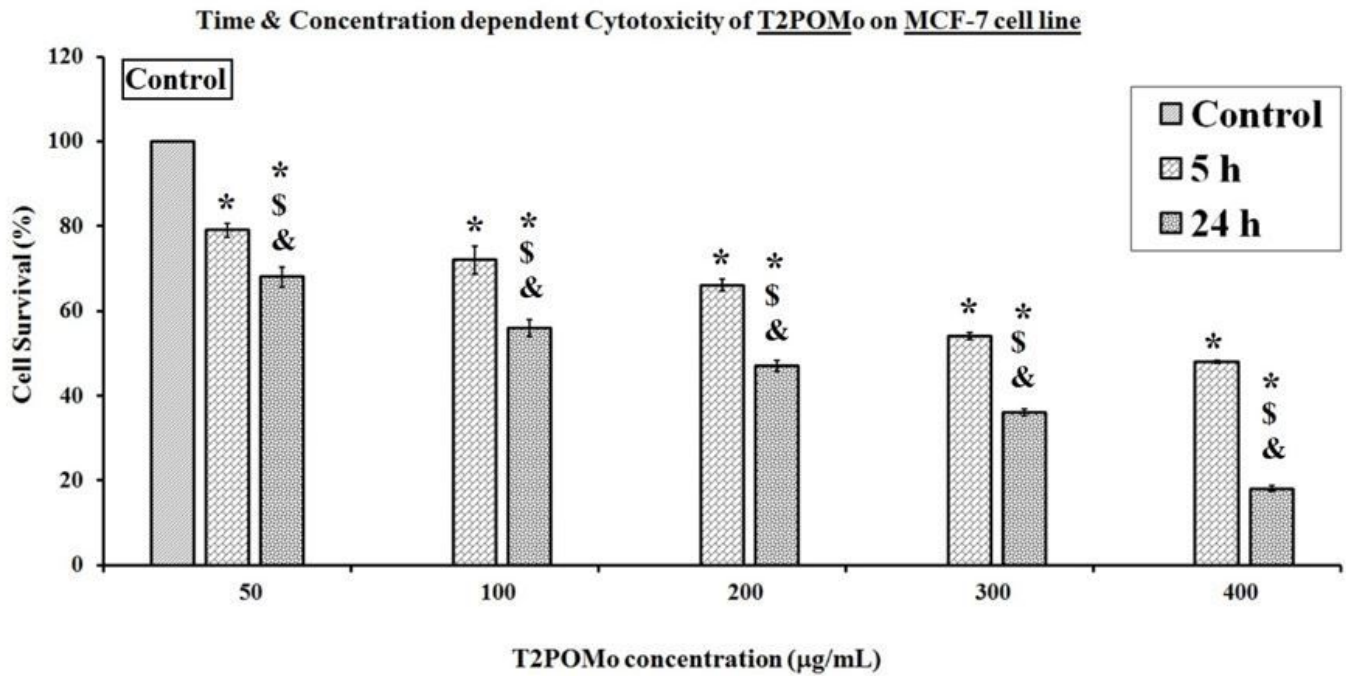


Figure 6

Stability of T2POMo chemical structure in PBS in freshly prepared solution and follow up to 72 h.



**Figure 7**

Time and dose dependent cytotoxicity of T2POMo bioconjugate on MCF-7 cell line \*: means the significant difference with control group ( $p < 0.05$ ) \$ refers to significant difference between different time of incubations ( $p < 0.05$ ) & refers to significant difference between different concentrations ( $p < 0.05$ )

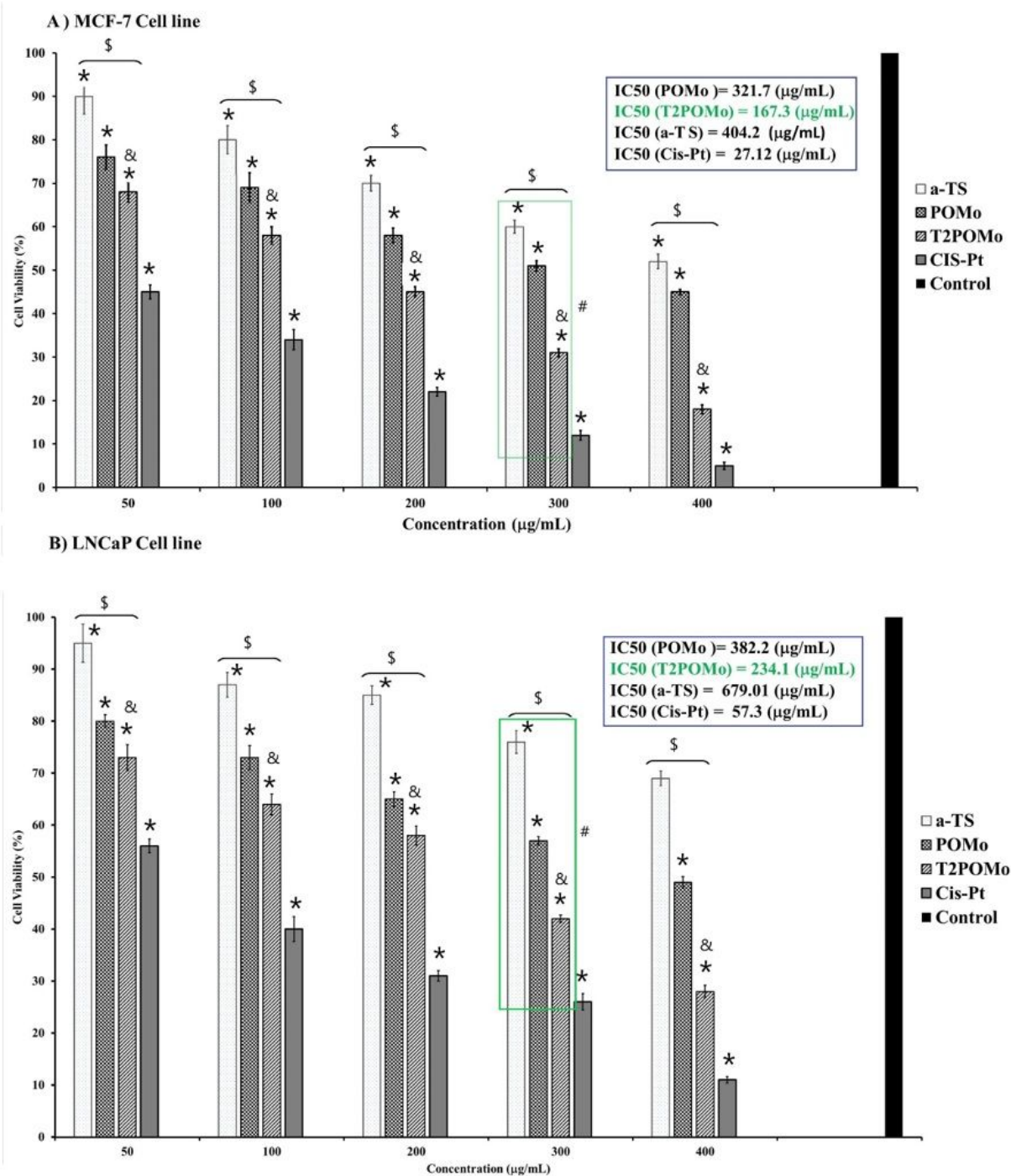


**Figure 8**

the comparative cytotoxicity of T2POMo and POM on the MCF-7 & LNCaP cell lines. In each diagram \* refers to significant difference with control; & refers to significant difference between POMo and T2POMo in each treated concentration; \$ refers to significant difference between each concentration set; and # refers to significant difference between POMo and T2POMo cytotoxicities and positive control Cis-Pt;  $p < 0.05$  was considered as significant difference.

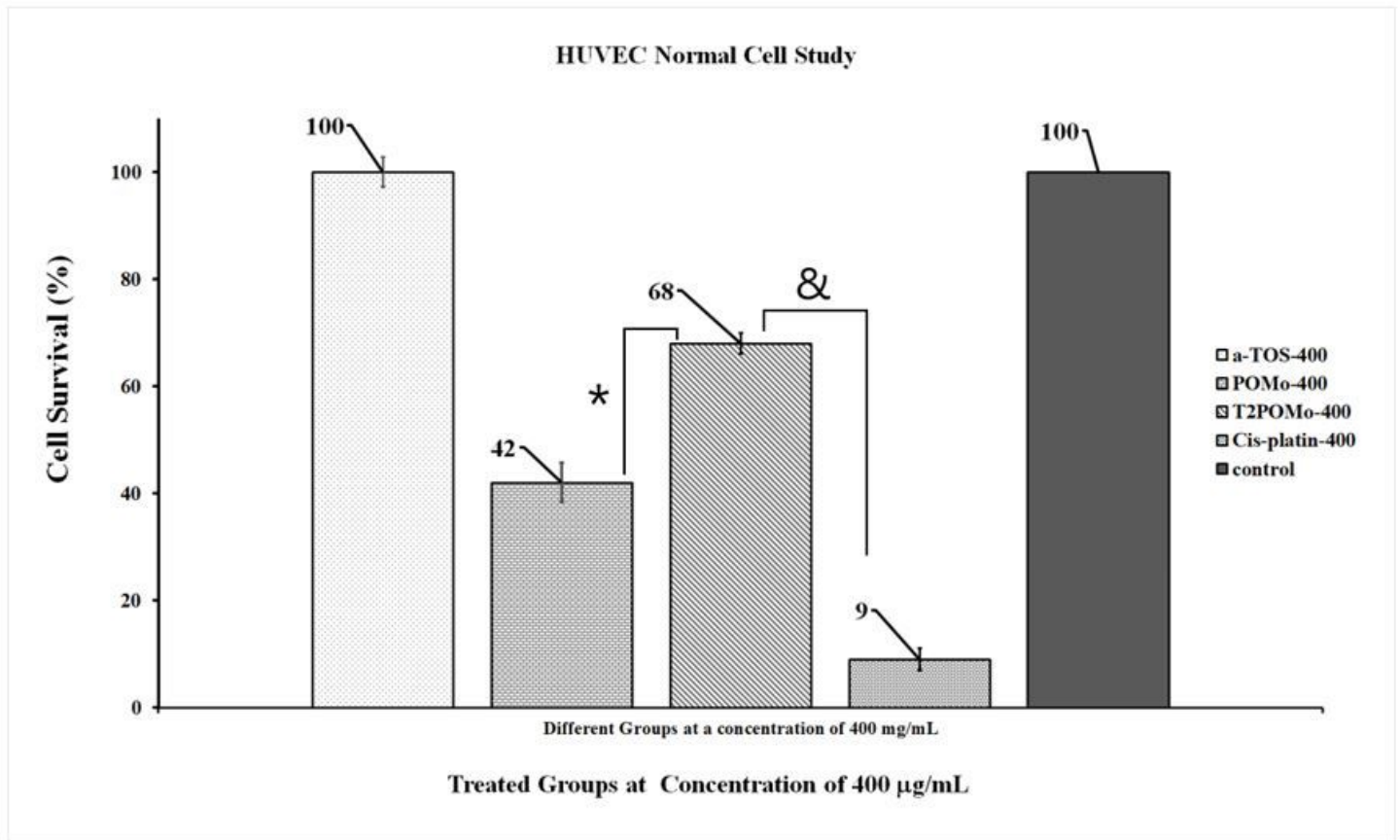


**Figure 9**

the comparative cytotoxicity of T2POMo, a-TS, and POM on the HUVEC cell line compare to the Cis-platin at the concentration of 400 µg/mL and control untreated cells (\* refers to significant difference between POMo and T2POMo results, & refers to significant difference between cytotoxicity of T2POMo and Cis-Platin; Pvalue < 0.05)

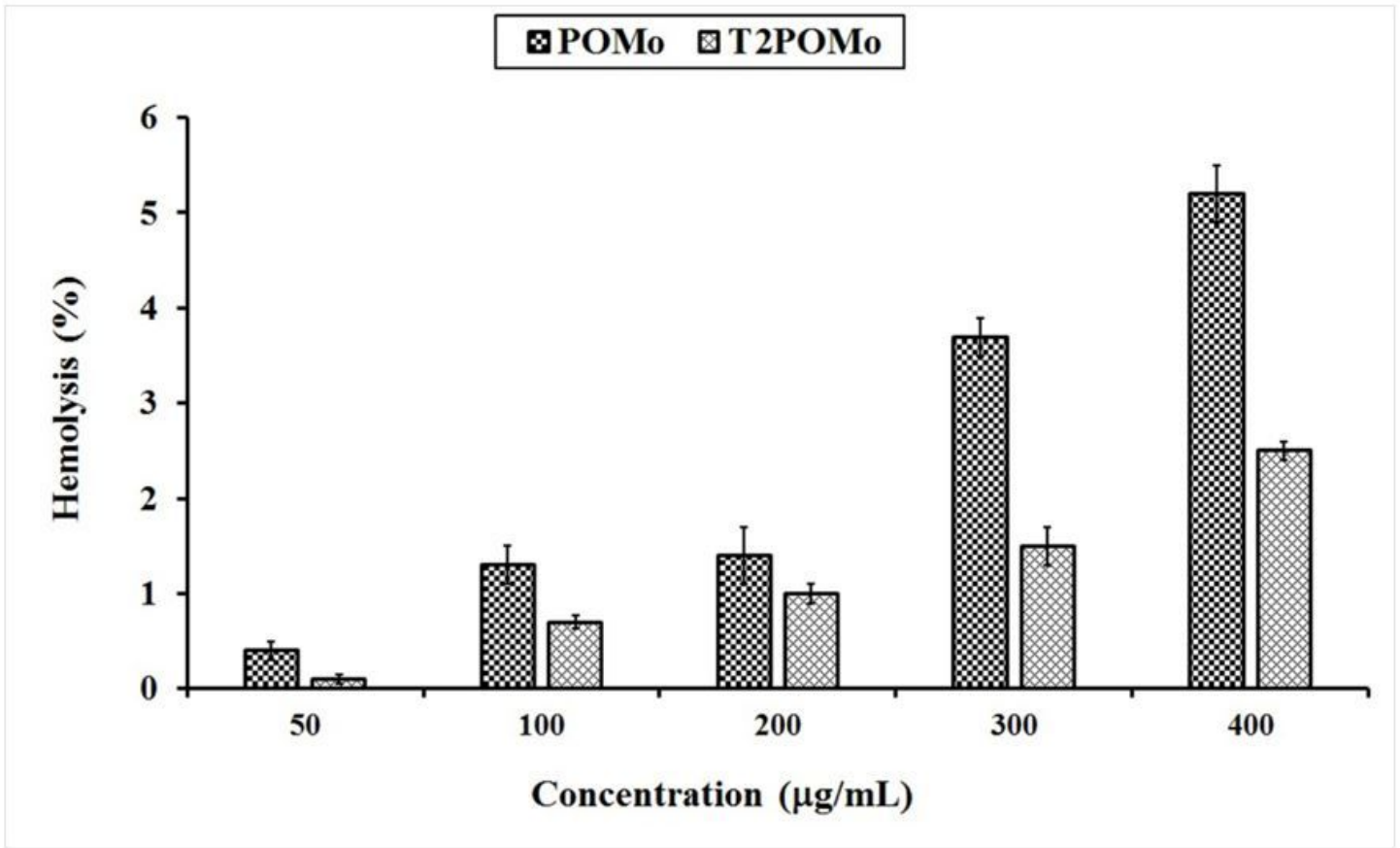


Figure 10

Hemolysis activity of POMo & T2POMo

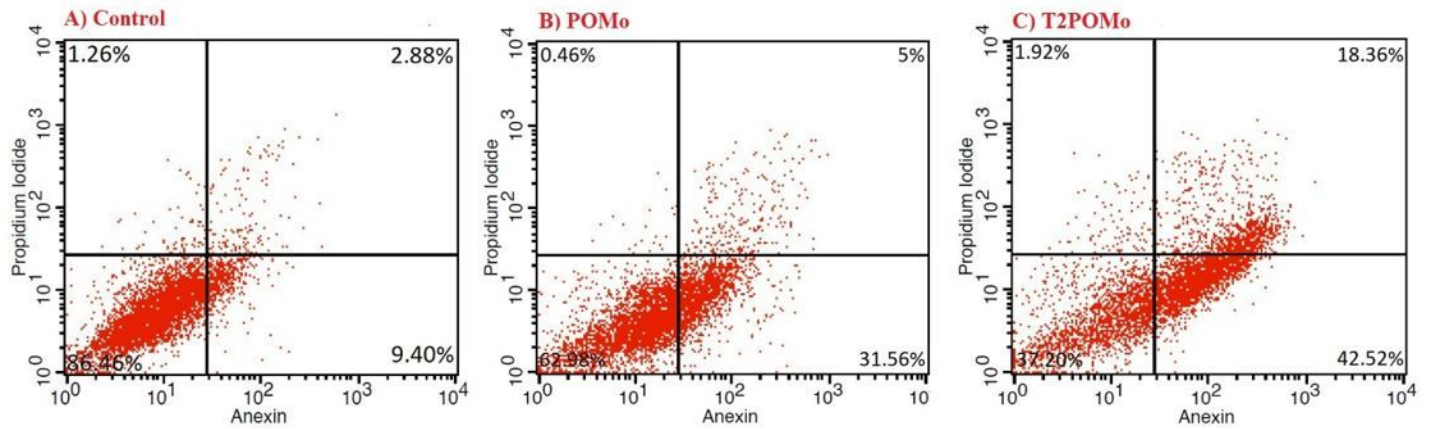


Figure 11

Annexin V/PI analysis of apoptosis in MCF-7 cancer cells induced by POMo & T2POMo